NASA TECHNICAL NOTE

NASA TN D-5535

NASA TN D-5535

A STRUCTURAL MERIT FUNCTION FOR AERODYNAMIC DECELERATORS

by Melvin S. Anderson, Herman L. Bohon, and Martin M. Mikulas, Jr.

Langley Research Center
Langley Station, Hampton, Va.

NATIONAL AERONAUTICS AND SPACE ADMINISTRATION • WASHINGTON, D. C. • NOVEMBER 1969

1. Report No. NASA TN D-5535	2. Government Accession No.	3. Recipient's Catalog No.
4. Title and Subtitle A STRUCTURAL MERIT FUNCTION FOR AERODYNAMIC DECELERATORS		5. Report Date November 1969 6. Performing Organization Code
7. Author(s) Melvin S. Anderson, Herman L. Bohon, and Martin M. Mikulas, Jr.		8. Performing Organization Report No. L-5605 10. Work Unit No. 124-07-23-01-23
9. Performing Organization Name and Address NASA Langley Research Center Hampton, Va. 23365		11. Contract or Grant No. 13. Type of Report and Period Covered Technical Note
12. Sponsoring Agency Name and Address National Aeronautics and Space Administration Washington, D.C. 20546		14. Sponsoring Agency Code

15. Supplementary Notes

16. Abstract

Equations for the mass of decelerators based on structural and aerodynamic considerations including the effects of minimum-gage material have been derived, and a suitable function representing decelerator efficiency has been identified. Equations for the merit function are presented for subsonic and supersonic parachutes, ballutes, and attached inflatable decelerators (AID). In the subsonic range three types of parachutes are compared and the ringsail was determined to be most efficient. In the supersonic range the ringsail was again most efficient for small sizes or low loading conditions, but the AID showed potential of efficiency comparable to the ringsail for large sizes or high loads. Application of the merit function to determine optimum deployment conditions for a planetary entry mission is also illustrated.

17. Key Words Suggested by Author(s)	18. Distribution Statement
Decelerators; Parachutes Decelerator weight analysis Inflatable structures Optimum deployment conditions	Unclassified – Unlimited

19. Security Classif. (of this report)	20. Security Classif. (of this page)	21. No. of Pages	22. Price*
Unclassified	Unclassified	33	$3.00

*For sale by the Clearinghouse for Federal Scientific and Technical Information
Springfield, Virginia 22151

A STRUCTURAL MERIT FUNCTION FOR AERODYNAMIC DECELERATORS

By Melvin S. Anderson, Herman L. Bohon,
and Martin M. Mikulas, Jr.
Langley Research Center

SUMMARY

Equations for the mass of decelerators based on structural and aerodynamic considerations including the effects of minimum-gage material have been derived, and a suitable function representing decelerator efficiency has been identified. Equations for the merit function are presented for subsonic and supersonic parachutes, ballutes, and attached inflatable decelerators (AID). In the subsonic range three types of parachutes are compared and the ringsail was determined to be most efficient. In the supersonic range the ringsail was again most efficient for small sizes or low loading conditions, but the AID showed potential of efficiency comparable to the ringsail for large sizes or high loads. Application of the merit function to determine optimum deployment conditions for a planetary entry mission is also illustrated.

INTRODUCTION

There is a growing need for aerodynamic decelerators that can operate over a wide speed range. Parachutes are widely used to decelerate payloads at subsonic speeds, and the development of supersonic configurations has produced a variety of canopy shapes which differ widely in structural and aerodynamic efficiency. The determination of the best decelerator for a given application involves detailed evaluation of the candidate systems. Thus, a simple means of comparing decelerator efficiency is desirable for use in such a preliminary design phase when trade-off studies are made. In the present paper, an appropriate merit function is developed from the general equations relating decelerator mass and drag to the applied loading. This merit function is a measure of relative efficiency for decelerators and is independent of decelerator size.

Several configurations are compared on the basis of the proposed merit function. Both subsonic and supersonic devices are considered, including ballutes, attached inflatable decelerator (AID), and several types of parachutes. The effect of minimum-gage construction is included. A simplified method for determining optimum deployment conditions for a given planetary entry design problem is illustrated.

SYMBOLS

The units for the physical quantities defined in this paper are given both in the U.S. Customary Units and in the International System of Units, SI. Appendix A presents factors relating these two systems of units.

A	total projected area of decelerator
A_b	surface area of burble fence
A_f	surface area of pressure-vessel canopy
A_o	surface area of parachute canopy
a,b,c	constants
C_D	drag coefficient based on total projected area
C_{D_o}	drag coefficient based on nominal diameter D_o
D_o	nominal diameter of parachute, $\sqrt{4A_o/\pi}$
d_f	canopy mass per unit area
F_s	suspension-line strength
f	fabric stress resultant (load per unit length)
$\bar{f}$	nondimensional fabric stress resultant, $2f/PR$
f_a	allowable fabric stress resultant
K_C	construction factor
K_D	design factor
k_c	strength-mass ratio of suspension lines, F_s/γ
k_f	strength-mass ratio of fabric, f_a/d_f

l_m	length of meridian cord
l_s	length of suspension line
l_t	length of towline
m	mass
m_T	total entry vehicle mass
n	number of meridian cords
P	internal pressure minus base pressure
p	pressure
q	free-stream dynamic pressure
$\bar{q}$	effective dynamic pressure at deployment accounting for shock load
R	maximum radius normal to axis of revolution including burble fence (see fig. 4)
R'	radius of canopy
r	radius of burble fence
T	meridian cord load
$\overline{T}$	nondimensional meridian cord load, $nT/P\pi R^2$
z	number of suspension lines
α	proportionality constant relating number of suspension lines to parachute diameter
β	factor accounting for stress increase due to lobing
γ	mass per unit length

η ratio of burble fence diameter to canopy diameter, $\frac{R - R'}{2R'}$

θ confluence angle of suspension lines

λ geometric porosity

ξ ratio of aeroshell radius to total decelerator radius

ρ ratio of length of suspension-line loop to length of suspension line

Subscripts:

d deployed

e entry

DEVELOPMENT OF PARAMETERS

The development of efficient aerodynamic decelerator systems requires the input of both aerodynamic and structural disciplines. Ideally a decelerator should have both a low structural mass and high drag coefficient, while providing stable aerodynamic performance. A suitable merit function should relate the structural and aerodynamic parameters which determine the decelerator efficiency.

From structural strength analysis the general form of the equation for mass of a tension structure is

$$m = bpR^3 \tag{1}$$

where b is a constant, p is some reference pressure loading, and R is a reference length. Equation (1) is generally applicable to the suspension and riser lines and meridian tapes used in deployable decelerators. However, if mass of the canopy fabric is based solely on equation (1), gages may result that are thinner than can be produced or used. Thus, it is convenient to express the total mass of a decelerator as

$$m = bpR^3 + cR^2d_f \tag{2}$$

where on the right the first term is the mass of meridian tapes and riser and suspension lines whereas the second term is the canopy mass. The canopy mass is proportional to the decelerator area (through R^2) and the fabric mass per unit area d_f. The fabric

thickness must always be equal to or greater than some minimum gage and may be a function of deployment or steady-state load requirements. Equation (2) can be put in a form suitable to reflect deceleration efficiency as follows: Taking R as the radius associated with the drag area and dividing equation (2) by C_DA gives

$$\frac{m}{C_DA} = bq\left(C_DA\right)^{1/2} + cd_f \tag{3}$$

where the constants b and c have been redefined. The reference pressure p is taken as the design dynamic pressure q. For designs where little deceleration occurs during deployment (the so-called infinite mass payload), q is the deployment dynamic pressure. However, in many instances, particularly at subsonic speeds, significant deceleration occurs during deployment so that the design dynamic pressure is less than that at deployment.

Equation (3) gives the decelerator mass as a function of the two principal design requirements, drag area and dynamic pressure. The first terms, representing suspension and riser lines and meridian tapes, is an explicit function of $q\left(C_DA\right)^{1/2}$. In appendix B it is shown that d_f also can be expressed as a function of $q\left(C_DA\right)^{1/2}$ for a wide variety of decelerators over the entire design range from minimum gage to strength limited. Thus, the most efficient decelerator will have the least value of m/C_DA for a given value of $q\left(C_DA\right)^{1/2}$, and m/C_DA is a proper merit function for decelerators if presented as a function of the single parameter $q\left(C_DA\right)^{1/2}$.

APPLICATION OF THE MERIT FUNCTION

Decelerator Efficiency

Equations of the form of equation (3) are derived in appendix B for several decelerator configurations. The characteristics of the structural merit function for decelerators are illustrated in the following sections by comparisons of the efficiency of several decelerator configurations.

Subsonic decelerators.- The merit function has been calculated for the three subsonic parachutes shown in figure 1: the ringsail, the hemisflo, and the flat circular. Results from equation (B4) are shown in figure 2 where $m/C_{D_o}A_o$ is plotted against $q\left(C_{D_o}A_o\right)^{1/2}$. The material was assumed to be the same (dacron at room-temperature strength) for all configurations in order to make direct comparisons between configurations. The canopy mass per unit area d_f is obtained from figures 3(a), 3(b), and 3(c) which show canopy strength requirements as a function of $q\left(C_{D_o}A_o\right)^{1/2}$. The value

of d_f is determined from these results and the strength-mass ratio of the fabric k_f. The solid curves were obtained from empirical relationships that have been developed in parachute design (ref. 1). The horizontal dash lines correspond to a minimum-gage canopy of 1.1 ozm/yd^2 (37.3 g/m^2) for cloth canopies and 1.83 ozm/yd^2 (62.0 g/m^2) for ribbon canopies. The development of the curves of figure 3 is given in appendix B.

The ringsail is shown in figure 2 to have the least mass for all values of $q\left(C_{D_o}A_o\right)^{1/2}$. At low values of $q\left(C_{D_o}A_o\right)^{1/2}$ the flat circular parachute is more efficient than the hemisflo because of different minimum gages. (See figs. 3(a) and 3(c).) The positions are reversed at higher values of $q\left(C_{D_o}A_o\right)^{1/2}$ where designs are governed by strength, because the flat circular parachute has higher opening shock loads than the hemisflo.

The results shown in figure 2 illustrate the general character of equation (3). At small values of q or C_DA the decelerator mass is controlled by minimum-gage considerations and the curves are almost horizontal. At higher values of $q\left(C_DA\right)^{1/2}$ the curves approach a slope of 1 and the design is strength limited. Another approach is to present decelerator mass as a function of q only. At low values of q mass is proportional to C_DA because of minimum-gage constraints; at high values of q mass is proportional to $\left(C_DA\right)^{3/2}$ because of strength requirements. Thus a suitable merit function independent of decelerator size would have to vary from m/C_DA to $m/\left(C_DA\right)^{3/2}$ as q increased or, conversely, if one parameter were selected it would be a function of size for certain ranges of q. Expressions equivalent to the form of the merit function $m/\left(C_DA\right)^{3/2}$ for strength-limited designs have been mentioned in references 2 to 5. However, the use of m/C_DA as a function of $q\left(C_DA\right)^{1/2}$ allows the full range of design conditions to be covered by a single curve. It is not expected that actual detail designs would result in a unique curve but they should fall in a rather narrow band for the same design criteria. Thus the parameters m/C_DA and $q\left(C_DA\right)^{1/2}$ allow reasonable comparison with other designs and the relative efficiency of a particular design can be determined.

Supersonic decelerators.- Development of parachutes which are stable at supersonic speeds has required modifications of the subsonic design. For example, in reference 1 it is indicated that the hemisflo parachute can be made stable by increasing the porosity and suspension-line length. However, these modifications are detrimental to efficiency since they cause decreases in drag coefficient and increases in structural weight. To avoid these penalties, various blunt ram-air-inflated devices have been considered such as the towed ballute described in reference 6 and the attached inflatable decelerator (AID) described in reference 2. Sketches of these devices and the supersonic hemisflo parachute are shown in figure 4.

Values of m/C_DA were calculated for the decelerators shown in figure 4 from the equations of appendix B, and the results are shown in figure 5. Results are also shown for subsonic ringsail configuration since recent flight tests (refs. 7 and 8) have shown that subsonic parachutes (namely, the ringsail and disk gap band) may be used at Mach numbers up to 2 and at low dynamic pressures (of the order of 10 psf (480 N/m^2)). Material properties for nomex at 350^o F (450 K) were used for all configurations since some aerodynamic heating may be expected. The canopy mass per unit area is determined from figures 3(b) and 3(c) for the parachutes, figure 3(d) for the ballute, and figure 3(e) for the AID. The minimum gage for the ram-air-inflated decelerators corresponds to 2.3 ozm/yd^2 (78 g/m^2) which includes 0.5 ozm/yd^2 (17 g/m^2) for coating to reduce porosity to acceptable levels. Two curves are shown for the ballute. The lower curve represents the ideal mass based on theoretical load requirements when the ballute is fully inflated. Design and testing experience has indicated that somewhat heavier canopies are required to prevent failure due to flagging during deployments, and the upper curve reflects this experience. (See appendix B.) The drag coefficient used for the ringsail parachute was 0.65, which tends to be confirmed experimentally in reference 8 for Mach numbers up to 1.5. The length of suspension lines was unchanged from the subsonic configuration.

As can be seen from figure 5, the relative efficiency of the various devices is strongly dependent on the dynamic pressure of deployment. At low values of $q(C_DA)^{1/2}$ the subsonic ringsail parachute is the most efficient. In this region the AID is penalized by its higher minimum-gage requirements. The hemisflo is penalized at all values of $q(C_DA)^{1/2}$ by the low C_D and long suspension lines necessary for stability. The ballute is generally the least efficient configuration shown. However, more success has been achieved with the ballute in obtaining stability at the higher Mach numbers than with the parachute. (See ref. 6.)

The AID is in some respects similar to the ballute. However, the absence of a towline, a higher drag coefficient, and less surface area all lead to a more efficient configuration than the ballute. At the higher values of $q(C_DA)^{1/2}$ the AID is indicated as the most efficient of all configurations. However, these results have not been confirmed experimentally. In particular, the canopy gage may have to be increased beyond that required in the steady-state load condition to allow for the dynamics of deployment.

Correlation of the merit function for recent parachute designs with the merit-function curve is shown in figure 6. The parachutes, represented by the circles, were designed and tested in the NASA Planetary Entry Parachute Program (PEPP). (See ref. 8.) Details of the designs are given in references 9 to 12. The parachutes include two ringsails and two disk gap bands. The mass of the parachutes includes all mass from the canopy to the confluence of the suspension lines; $C_{D_o}A_o$ is based on a value

of C_{D_o} of 0.65 and the surface area associated with the canopy diameter D_o. The maximum dynamic pressure at deployment was evaluated as the design deployment load divided by $C_{D_o}A_o$. Since the design deployment load already includes any shock factors expected, the curve is shown for a shock factor of 1.0. The only other change from the curve shown in figure 5 is that the design factor is 2, the value corresponding to the design criteria of references 9 to 12. As can be seen from figure 6, the curve is in fair agreement with all four designs.

Determination of Optimum Deployment Conditions

Mission studies of entry into the thin Martian atmosphere have shown that size limitations on the entry capsule can severely limit the entry mass unless drag augmentation is provided during the supersonic portion of the entry. (See refs. 3 and 7.) Either the entry mass must be small or the drag significantly increased to achieve low enough velocities for typical mission requirements. If a specified altitude-velocity combination is a design goal, the merit function can be used to identify the optimum deployment conditions from the trajectory calculations. This problem is illustrated in figure 7. The inset figure shows a typical altitude-velocity plot for a given entry ballistic coefficient $m_T/(C_DA)_e$. The solid curve in the inset is for the entry vehicle alone and indicates that drag augmentation is required to achieve the design goal represented by the circle. Additional drag area may be deployed anywhere along the trajectory above the desired altitude. The curves show the amount of drag area required as a function of the dynamic pressure at deployment to achieve Mach 1 at an altitude of 15 000 ft (4570 m) for an entry velocity of 12 000 ft/sec (3660 m/s) and an entry angle of -15^o. An estimated lower bound of the Martian atmosphere surface pressure of 5 millibars (500 N/m^2) was used (VM-8 of ref. 13). The curves were obtained from trajectory studies by James F. McNulty, Daniel B. Snow, and Leonard Roberts conducted at Langley Research Center as part of a general mission study. These results are not necessarily applicable to an actual mission but they are realistic enough to give the proper trends. If deployment occurs at high altitudes, only a small decelerator is required; however, the dynamic pressure is high (point A in fig. 7). If deployment occurs at low altitude, the dynamic pressure is low but a large drag area is required (point B in fig. 7). Both of the extreme situations lead to a large decelerator mass and, obviously, somewhere in between is the optimum condition. The optimum deployment condition is defined as that value of q giving least decelerator mass for a given entry ballistic coefficient and can be found as follows. The curves presented in figure 5 for the mass of supersonic decelerators can be approximated by a series of straight lines, each with an equation of the type

$$\frac{m}{C_DA} = a\left[q(C_DA)^{1/2}\right]^s \tag{4}$$

where s is the slope of the curve. If an equation of this type is applicable over the range of possible sizes and dynamic pressures, it is simple to make the proper trade off between C_DA and q. The optimum decelerator is that which has the least value of $\left[q(C_DA)^{1/2}\right]^s C_DA$. In figure 5, most of the curves exhibit a slope s of about 1 beyond $q(C_DA)^{1/2}$ of 300 lbf/ft (4.4 kN/m), the region of interest for the requirements indicated by figure 7 for entry vehicles with diameter greater than about 10 ft (3 m). Thus, for this case, the optimum decelerator has the least value of $q(C_DA)^{3/2}$ for a given entry ballistic coefficient. The results of this optimization are shown in figure 8 where the deployed-decelerator area $(C_DA)_d$ that leads to least-mass decelerators is plotted as a function of entry ballistic coefficient. The Mach number at deployment is shown by the tick mark on the curve.

The maximum allowable ballistic coefficient if no decelerator is deployed is approximately 0.25 slug/ft^2 (39 kg/m^2) $\left((C_DA)_d/(C_DA)_e = 1\right)$. Significant increases in landed mass for a given size can be made (up to a factor of 3 for this example) by supersonic deployment of a decelerator. The curve indicates the optimum decelerator area and the corresponding deployment Mach number for a given entry ballistic coefficient.

The method described can be used to determine optimum deployment conditions without detailed knowledge of the decelerator. Optimum conditions do not depend on the magnitude of decelerator mass but only on the trend of m/C_DA with $q(C_DA)^{1/2}$. For example, if the results are in the minimum-gage range, the exponent on $q(C_DA)^{1/2}$ can be suitably modified to reflect the slope of m/C_DA plotted against $q(C_DA)^{1/2}$.

CONCLUDING REMARKS

A structural merit function for aerodynamic deceleration systems has been developed which relates the decelerator mass required to the desired drag area and design loading condition. These quantities are combined in the form m/C_DA given as a function of $q(C_DA)^{1/2}$ where m is the decelerator mass, C_DA is the drag area, and q is design dynamic pressure. This form of presentation results in a single curve independent of decelerator size including the minimum-gage region as well as the strength-limited region.

Several subsonic and supersonic parachute configurations as well as two ram-air-inflated devices were compared on the basis of the merit function. The ringsail parachute was the most efficient subsonic decelerator and was also the most efficient in the supersonic range for most of the design range. The attached inflatable decelerator (AID) was the most efficient supersonic decelerator at higher values of $q(C_DA)^{1/2}$ but tests are required to determine whether the indicated mass requirements are achievable. The

results presented should be useful as a standard for comparison with other decelerator designs on the basis of the merit function.

The simplicity of the merit function is illustrated with a typical planetary entry mission problem. For a specified goal of an altitude-velocity combination and entry ballistic coefficient the optimum deployment Mach number and required decelerator drag area are readily determined, without regard to details of a decelerator configuration. The use of this merit function would be a considerable asset in early mission trade-off studies.

Langley Research Center,
National Aeronautics and Space Administration,
Langley Station, Hampton, Va., August 27, 1969.

APPENDIX A

CONVERSION OF U.S. CUSTOMARY UNITS TO SI UNITS

The international System of Units (SI) was adopted by the Eleventh General Conference on Weights and Measures, Paris, October 1960 (ref. 14). Conversion factors for the units used herein are given in the following table:

Physical quantity	U.S. Customary Unit	Conversion factor (*)	SI Unit
Area	ft^2	0.0929	square meters (m^2)
	yd^2	0.8361	square meters (m^2)
Force	lbf	4.448	newtons (N)
Mass	lbm	0.4536	kilograms (kg)
	ozm	0.0283	kilograms (kg)
	slug	14.59	kilograms (kg)
Length	ft	0.3048	meters (m)
Pressure	psf = lbf/ft^2	47.88	newtons/$meter^2$ (N/m^2)
	millibar	100	newtons/$meter^2$ (N/m^2)
Velocity	ft/sec	0.3048	meters/second (m/s)
Temperature . .	$^oF + 459.67$	5/9	kelvins (K)

*Multiply value given in U.S. Customary Unit by conversion factor to obtain equivalent value in SI Unit.

The prefix used to indicate multiples of units is as follows:

Prefix	Multiple
kilo (k)	10^3

APPENDIX B

DECELERATOR MASS EQUATIONS

In this appendix, equations for the decelerator merit function are presented for several decelerators of the subsonic type and the supersonic type. The equations include both strength-limited designs and minimum-gage designs for the basic drag-producing surface. Equations make use of current design practice and experience whenever available. The development of the equations for the structural mass is shown to give some indication of the assumptions involved.

Subsonic Decelerators

Subsonic parachutes have evolved to the point where semiempirical equations may be used to obtain reliable designs. Three typical subsonic parachutes are shown in figure 1. The primary mass components of parachutes are the canopy fabric and the suspension lines. Of the configurations shown the flat circular parachute has a solid cloth canopy whereas the hemisflo parachute has a ribbon canopy. The ringsail parachute has wide rings of cloth in its canopy. In the design of parachutes, suspension-line strength requirements can be predicted accurately from the drag force, and the lines are rarely minimum gage; however, canopy strength requirements are not amenable to simple analysis. For this reason the canopy strength will be estimated on the basis of suspension-line strength – an empirical procedure discussed in reference 1.

The total mass of parachutes is written as the mass of the component parts. Thus

$$m = \gamma \frac{z}{2} \rho l_s + K_C d_f A_o (1 - \lambda) \tag{B1}$$

where γ is the mass per unit length of the suspension lines and radial tapes. The total number of suspension-line loops is $z/2$ with an equivalent length ρl_s. The canopy mass (last term in eq. (B1)) includes the construction factor K_C, the mass per unit area d_f, the surface area A_o, and the geometric porosity λ. The construction factor accounts for excess material mass due to seam overlap, lobing, and thread mass.

In the suspension-line term of equation (B1) the mass per unit length γ is defined as the allowable load of each suspension line divided by its strength-mass ratio, or

$$\gamma = \frac{F_s}{k_c} = \frac{K_D}{4 \cos \theta} \frac{\bar{q}}{q} \frac{\pi C_{D_o} D_o^2}{k_c z} q \tag{B2}$$

where $\bar{q}/q$ is the opening shock factor, C_{D_o} is the drag coefficient associated with the nominal diameter D_o, θ is the confluence angle of the suspension lines, and K_D is a design factor which accounts for the safety factor, seam and joint efficiency, abrasion, moisture, and fatigue (see p. 370 of ref. 1). Substitution of equation (B2) into (B1) gives

$$m = \frac{K_D}{8 \cos \theta} \frac{\bar{q}}{q} \frac{\rho l_s}{D_o} \frac{\pi C_{D_o} D_o^3}{k_c} q + K_C d_f A_o (1 - \lambda) \tag{B3}$$

The form of the merit function used in the text is obtained by dividing equation (B3) by $C_{D_o} A_o$. Thus,

$$\frac{m}{C_{D_o} A_o} = \frac{K_D}{\pi^{1/2} \cos \theta} \frac{\bar{q}}{q} \frac{\rho l_s}{D_o} \frac{1}{k_c C_{D_o}^{1/2}} q \left(C_{D_o} A_o\right)^{1/2} + \frac{K_C}{C_{D_o}} (1 - \lambda) d_f \tag{B4}$$

Equation (B4) is of the form

$$\frac{m}{C_{D_o} A_o} = bq \left(C_{D_o} A_o\right)^{1/2} + cd_f \tag{B5}$$

where b and c are constants which depend on decelerator geometry and performance, but not on size.

Values of the parameters which make up the constants b and c of equation (B5) for subsonic decelerators are listed in table I. Where possible, the values tabulated are the results from design experience and can be found in reference 1. For example, the values of the shock factor $\bar{q}/q$, design factor K_D, and drag coefficient C_{D_o} are based on averages of a large number of full-scale tests. The values of the strength-mass parameters k_c and k_f are representative of dacron and nylon at room temperature. Radial tapes are considered herein as simple extensions of suspension lines which extend over the canopy; thus, the suspension-line loop ρl_s for subsonic parachutes is taken as $3D_o$.

Substituting values from table I for the parameters of equation (B4) yields the following design constants:

Subsonic parachute	b		c
	$\frac{\text{lbm}}{\text{lbf-ft}}$	$\frac{\text{kg}}{\text{N-m}}$	
Flat circular	12.5×10^{-5}	4.2×10^{-5}	1.79
Ringsail	6.6	2.2	1.67
Hemisflo	8.1	2.7	1.88

The design mass per unit area d_f (eq. (B5)) is difficult to establish with any degree of accuracy. Approximate values can be obtained from the correlation of canopy strength with suspension-line strength given in table 7-5 of reference 1 for ribbon canopy and table 7-6 for cloth canopy. It is also indicated that the number of suspension lines is proportional to the canopy diameter ($z = \alpha D_o$). With this relationship, the suspension-line strength may be expressed as a function of the loading parameter $q(C_DA)^{1/2}$ as follows:

$$F_s = \left[\frac{K_D}{\alpha \cos \theta} \frac{\bar{q}}{q}\left(\frac{\pi C_{D_o}}{4}\right)^{1/2}\right] q(C_{D_o}A_o)^{1/2} \tag{B6}$$

The parameters in the brackets are functions of parachute performance and are known for each type of parachute. Thus, with equation (B6) the canopy mass per unit area d_f can be correlated with the loading parameter $q(C_DA)^{1/2}$. This correlation is given in table II where α is 1.0 when D_o is given in feet.

In table II the cloth-canopy mass per unit area and ribbon-canopy strength listed for each value of suspension-line strength F_s are taken directly from reference 1. The cloth canopy d_f is representative of nylon or dacron with a room-temperature strength-mass ratio k_f shown in table I. The conversion of ribbon strength to ribbon d_f in table II is made by using the lightest nylon ribbon available for each strength requirement with the average value of ribbon strength-mass ratio k_f listed in table I. Also shown in table II are values of the loading parameter $q(C_DA)^{1/2}$ from equation (B6) which correspond to each value of F_s for the cloth canopies (flat circular and ringsail) and the ribbon canopy (hemisflo).

The results in table II are used to obtain figures 3(a), 3(b), and 3(c) where canopy allowable load f_a is plotted against the loading parameter for the subsonic parachutes of figure 1. The allowable load is the product of mass per unit area d_f and strength-mass ratio k_f. The circles represent data plotted from table II, and the curves faired through the data establish the trend of f_a with increases in $q(C_{D_o}A_o)^{1/2}$. The dash line is the minimum allowable load resulting from minimum-gage requirements. For cloth canopies the minimum d_f corresponds to 1.1 ozm/yd^2 (37.3 g/m^2) material. The

minimum gage for ribbon canopies is based on a minimum ribbon strength of 100 lbf (0.44 kN) (table II) which is correlated with a d_f of 1.83 ozm/yd^2 (62.0 g/m^2). The merit function plotted in figure 2 for the flat circular, ringsail, and hemisflo parachutes is based on d_f obtained from the curves in figure 3.

Supersonic Decelerators

Three decelerator configurations applicable in the supersonic speed range are shown in figure 4; they are a modified hemisflo parachute, a ballute, and an attached inflatable decelerator (AID). Whereas the hemisflo has geometric porosity to permit airflow through the canopy, the ballute and AID are pressure vessels which rely on internal pressure to stabilize the inflated shape. Thus, the ballute and AID require a thin coating on the fabric to maintain low permeability. Typical construction details of the modified hemisflo, AID, and ballute are found in references 1, 2, and 6, respectively. Equations for mass of these supersonic decelerators are developed in the next two sections.

Supersonic parachutes.- The use of parachutes at supersonic speed has been limited almost entirely to subsonic ribbon-type parachutes with appropriate modifications. A modification suggested in reference 1 for inflation stability is the increase in suspension-line length to twice the canopy nominal diameter D_o. Consequently, the total length of a suspension-line loop ρl_s is $5D_o$. This modification would not affect the basic mass equation; therefore, the merit function for the modified hemisflo parachute is the same as equation (B4). Values of the geometric and performance parameters which make up the constants b and c are listed in table I.

Pressure vessels.- The merit function for pressure-vessel-type decelerators is obtained in terms of parameters from reference 2, wherein an isotensoid analysis is employed to determine the aerodynamic shape. The components of total mass include the mass of the canopy and burble-fence fabric, meridian cord, and, for towed decelerators, the towline. The total mass is

$$m = n l_m \gamma + l_t \gamma + K_C d_f \left(A_f + A_b\right) \tag{B7}$$

where n is the number of meridian cords of length l_m, l_t is the towline length if required, A_f is the surface area of the canopy, and A_b is the surface area of the burble fence. It has been assumed that the same fabric is used for the burble fence and the canopy. Equation (B7) can be written as the merit function by using the nondimensional parameters of reference 2 as follows:

$$\frac{m}{C_D A} = \frac{K_D}{(C_D\pi)^{1/2} k_c (1 - \xi^2)^{3/2}} \left[\frac{P/q}{C_D} \frac{l_m}{R'} \frac{\bar{T}}{(1 + 2\eta)^3} + \frac{l_t}{R} \right] q (C_D A)^{1/2}$$

$$+ \frac{K_C}{C_D (1 + 2\eta)^2} \left[\frac{A_f}{\pi R'^2} + 4\pi\eta(1 + \eta) \right] \frac{d_f}{1 - \xi^2} \tag{B8}$$

The area of the decelerator includes the area of the burble fence, but excludes the area of the aeroshell in the case of the AID (see fig. 4). The parameter ξ is the ratio of aeroshell radius to total decelerator radius.

The fabric mass per unit area is the minimum gage or that required from strength considerations, whichever is greater. For the latter case, d_f is

$$d_f = \left[\frac{K_D \beta \bar{f}}{2(1 + 2\eta) k_f (C_D\pi)^{1/2}} \frac{P}{q} \right] q (C_D A)^{1/2} \tag{B9}$$

The factor β has been introduced to allow for an increase in fabric stress over the theoretical value f due to lobing.

A family of isotensoid shapes is presented in reference 2 for a given value of P/q and various values of $\bar{f}$ and $\bar{T}$. From these shapes the parameters $A_f/\pi R'^2$ and l_m/R' are obtained. Likewise, integration of the pressure distribution over the frontal area of the prescribed canopy shape yields an analytical value of C_D. The towline length is dependent primarily on the size and bluntness of the forebody or payload. Wind-tunnel studies have shown that towline lengths of 4 to 8 forebody diameters may be required to provide a stable configuration with high drag. (See ref. 15.)

Equation (B8) is of the general form as equation (3). The design constants b and c determined from table I are as follows:

Supersonic decelerator	b		c
	$\frac{\text{lbm}}{\text{lbf-ft}}$	$\frac{\text{kg}}{\text{N-m}}$	
Hemisflo	22.8×10^{-5}	7.6×10^{-5}	3.13
Ballute	20.6	6.9	7.41
AID	3.3	1.1	4.02

For supersonic application, nomex fabric and tapes with strength-mass ratio at 350° F (450 K) was used for comparison. The value of k_c for nomex at 350° F (450 K)

is about the same as for dacron at room temperature. The parameters in table I for the ballute and AID have been used in decelerator designs, and the drag coefficients C_D are average experimental values from tests at Mach numbers greater than 2. (See refs. 4, 16, and 17.)

The canopy mass per unit area d_f for the ballute and AID can be obtained from figures 3(d) and 3(e), respectively, by using the strength-mass ratios listed in table I. The strength-limited curve is obtained from equation (B9). The minimum-gage value of d_f was taken as 1.8 ozm/yd^2 (61 g/m^2) with an additional 0.5 ozm/yd^2 (17 g/m^2) coating to reduce porosity. The canopy is minimum gage over a large range of the loading parameter $q(C_DA)^{1/2}$ for both the ballute and AID as is evident from figures 3(d) and 3(e). A curve based on a criterion to prevent canopy failure during deployment of the ballute is also shown in figure 3(d). The criterion was developed to withstand flagging during deployment at subsonic speeds and has been applied to designs for supersonic deployment. (See ref. 18.) Comparison of the supersonic decelerators is made in figure 5 by use of the curve from figure 3 and the design constants from the preceding table.

REFERENCES

1. Anon.: Performance of and Design Criteria for Deployable Aerodynamic Decelerators. ASD-TR-61-579, U.S. Air Force, Dec. 1963.

2. Mikulas, Martin M., Jr.; and Bohon, Herman L.: Development Status of Attached Inflatable Decelerators. J. Spacecraft Rockets, vol. 6, no. 6, June 1969, pp. 654-660.

3. Guy, L. D.: Structural Design Options for Planetary Entry. AIAA Paper No. 68-344, Apr. 1968.

4. McShera, John T., Jr.; and Bohon, Herman L.: A Summary of Supersonic Decelerators With Emphasis on Problem Areas in Aerodynamics and Structures. AIAA Paper No. 67-201, Jan. 1967.

5. Anderson, Roger A.: New Horizons in Structural Design. AIAA/ASME Seventh Structures and Materials Conference, Apr. 1966, pp. 45-51.

6. Alexander, William C.; and Lau, Richard A.: State-of-the-Art Study for High-Speed Deceleration and Stabilization Devices. NASA CR-66141, 1966.

7. Gillis, Clarence L.: Aerodynamic Deceleration Systems for Space Missions. AIAA Paper No. 68-1081, Oct. 1968.

8. Murrow, Harold N.; and McFall, John C., Jr.: Summary of Experimental Results Obtained From the NASA Planetary Entry Parachute Program. AIAA Paper No. 68-934, Sept. 1968.

9. Stone, F. J.: 40-ft-Diameter Ringsail Parachute – Planetary Entry Parachute Program. NASA CR-66586, [1967].

10. Stone, F. J.: 55-ft-D_o Ringsail Parachute – Planetary Entry Parachute Program. NASA CR-66588, 1967.

11. Lemke, Reinhold: 40 ft DGB Parachute. NASA CR-66587, 1967.

12. Lemke, Reinhold A.; and Niccum, Ronald J.: 65 Foot Diameter D-G-B Parachute – Planetary Entry Parachute Program. NASA CR-66589, 1967.

13. Stone, Irving: Atmospheric Data to Alter Voyager Design. Aviat. Week Space Technol., vol. 83, no. 21, Nov. 22, 1965, pp. 66-67, 69.

14. Comm. on Metric Pract.: ASTM Metric Practice Guide. NBS Handbook 102, U.S. Dep. Com., Mar. 10, 1967.

15. McShera, John T., Jr.: Aerodynamic Drag and Stability Characteristics of Towed Inflatable Decelerators at Supersonic Speeds. NASA TN D-1601, 1963.

16. Reichenau, David E. A.: Investigation of an Attached Inflatable Decelerator System for Drag Augmentation of the Voyager Entry Capsule at Supersonic Speeds. AEDC-TR-68-71, U.S. Air Force, Apr. 1968.

17. Baker, D. C.: Investigation of an Inflatable Decelerator Attached to a 120-deg Conical Entry Capsule at Mach Numbers From 2.55 to 4.40. AEDC-TR-68-227, U.S. Air Force, Oct. 1968.

18. Barton, R. Reed: Development of Attached Inflatable Decelerators for Supersonic Application. NASA CR-66613, 1968.

TABLE I.- STRUCTURAL AND AERODYNAMIC PARAMETERS OF VARIOUS DECELERATORS

Parameter	Subsonic parachute			Supersonic decelerator			
	Flat circular	Hemisflo	Ringsail	Modified hemisflo parachute	Ringsail parachute	Ballute	AID
θ	20.5°	20.5°	20.5°	10.1°	20.5°	---	---
$\bar{q}/q$	2	1.1	1.1	1.5	1.1	1	1
k_c, $\frac{\text{lbf-ft}}{\text{lbm}}$	100 000	100 000	100 000	100 000	100 000	100 000	100 000
$\left(\frac{\text{N-m}}{\text{kg}}\right)$	(299 000)	(299 000)	(299 000)	(299 000)	(299 000)	(299 000)	(299 000)
k_f, $\frac{\text{lbf-ft}}{\text{lbm}}$	60 000	80 000	60 000	80 000	33 000	33 000	33 000
$\left(\frac{\text{N-m}}{\text{kg}}\right)$	(179 000)	(239 000)	(179 000)	(239 000)	(98 500)	(98 500)	(98 500)
K_D	2.9	2.9	2.9	2.9	2.9	2.9	2.9
K_C	1.25	1.25	1.25	1.25	1.25	1.25	1.25
C_{D_o}	0.7	0.5	0.75	0.3	0.75	---	---
C_D	---	---	---	---	---	0.63	1.06
P/q	---	---	---	---	---	2.4	2
$\overline{T}$	---	---	---	---	---	0.865	0.44
$A_f/\pi R'^2$	---	---	---	---	---	4	2.81
$\bar{f}$	---	---	---	---	---	0.135	0.09
η	---	---	---	---	---	0.1	0.05
$\rho l_s/D_o$	3	3	3	5	3	---	---
l_m/R'	---	---	---	---	---	π	2.56
l_t/R'	---	---	---	---	---	4	---
λ	0	0.25	0	0.25	0	---	---
ξ	---	---	---	---	---	0	0.40
β	---	---	---	---	---	2	2

TABLE II.- CORRELATION OF PARACHUTE SUSPENSION-LINE STRENGTH WITH CANOPY STRENGTH

(a) U.S. Customary Units

Suspension-line strength F_s, lbf	Cloth canopy			Ribbon canopy		
	d_f, lbm/ft^2	$q(C_DA)^{1/2}$, lbf/ft		Ribbon strength, lbf	d_f, lbm/ft^2	$q(C_DA)^{1/2}$, lbf/ft
		Flat circular	Ringsail			Hemisflo
375	0.76×10^{-2}	120	208	100	1.27×10^{-2}	255
550	1.11	175	305	200	1.67	374
1500	1.56	480	835	300	2.02	1020
2300	2.43	734	1280	500	4.45	1560
4000	3.30	1270	2220	1000	6.66	2720
6000	4.86	1910	3330			

(b) SI Units

Suspension-line strength F_s, kN	Cloth canopy			Ribbon canopy		
	d_f, g/m^2	$q(C_DA)^{1/2}$, kN/m		Ribbon strength, kN	d_f, g/m^2	$q(C_DA)^{1/2}$, kN/m
		Flat circular	Ringsail			Hemisflo
1.67	37.3	1.75	3.04	0.44	62.0	3.72
2.44	54.1	2.55	4.45	.89	81.5	5.45
6.67	76.1	7.00	12.20	1.33	98.5	14.90
10.02	118.5	10.70	18.70	2.22	217.0	22.80
17.80	161.0	18.50	32.40	4.45	325.0	39.70
26.70	237.0	27.80	48.60			

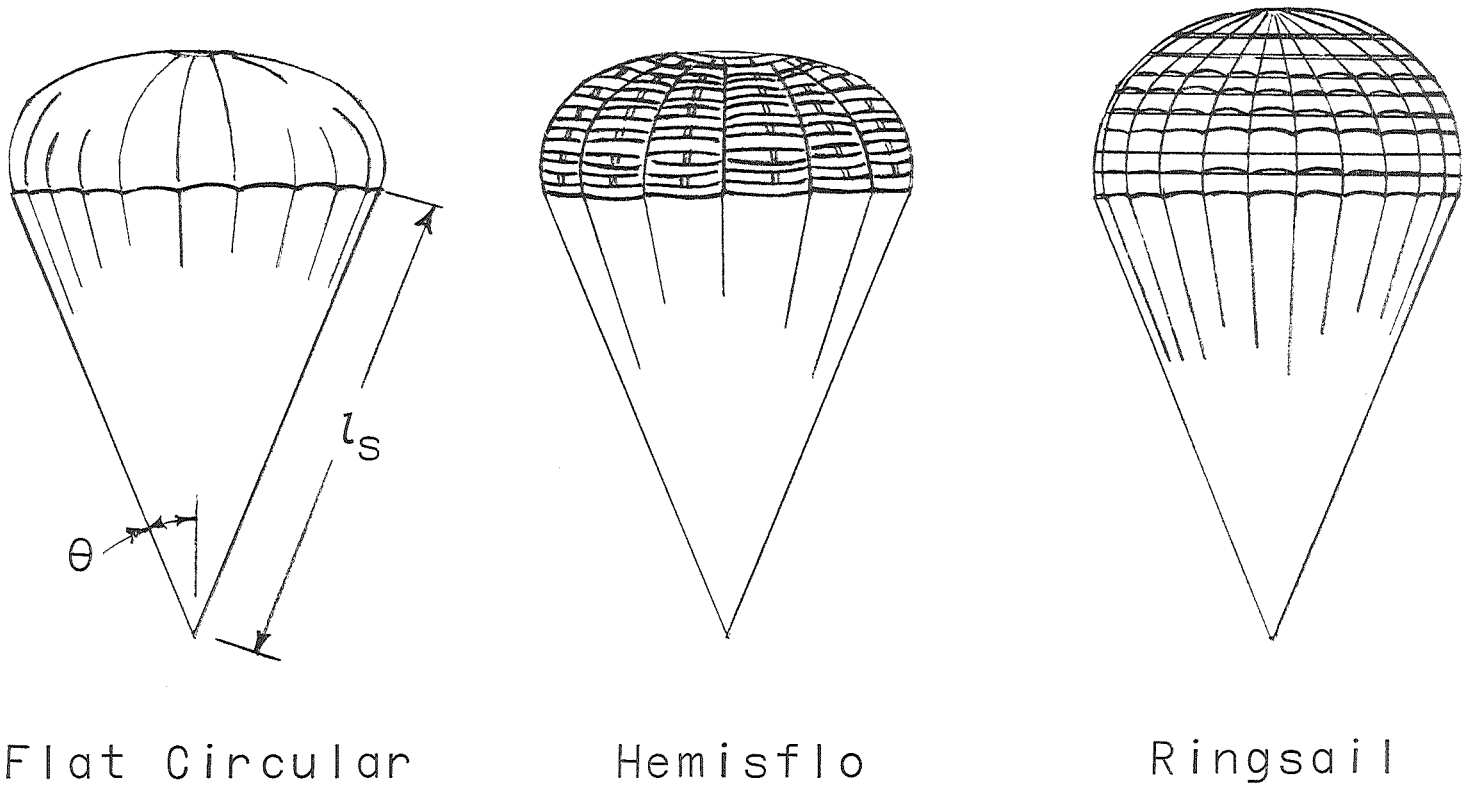

Figure 1.- Subsonic decelerators.

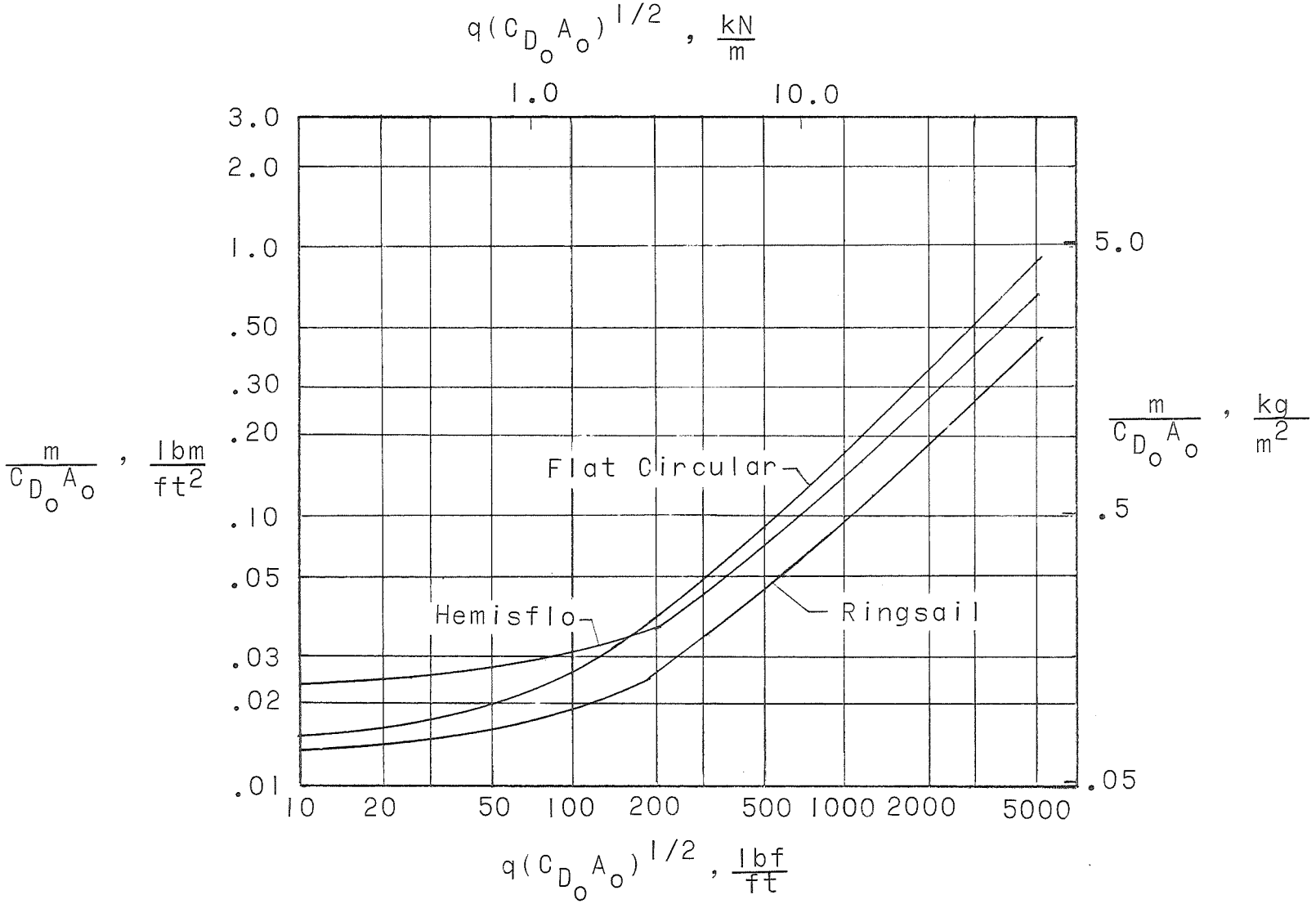

Figure 2.- Merit function for subsonic parachutes.

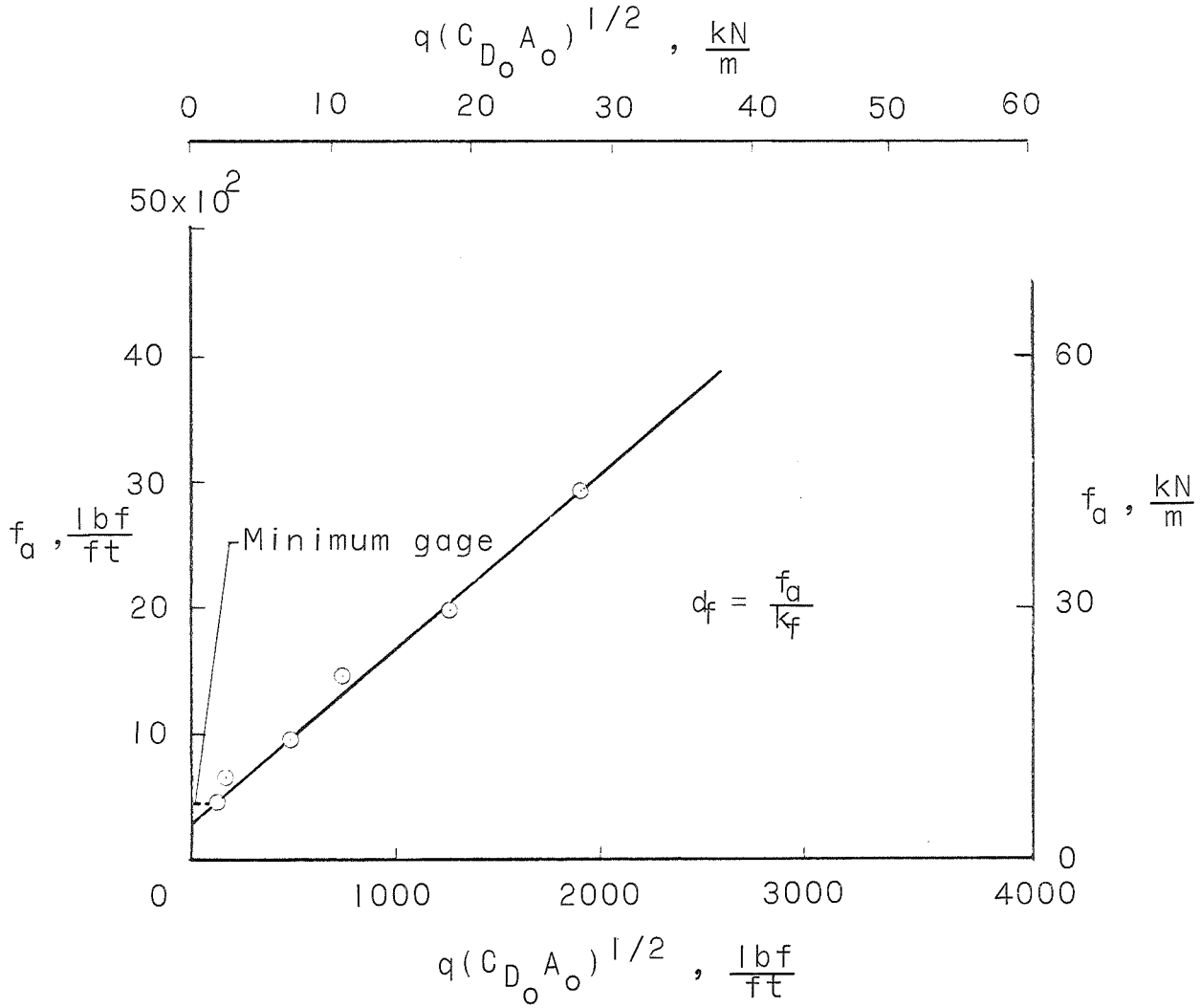

(a) Flat circular.

Figure 3.- Canopy allowable load as function of loading parameter. $d_f = \frac{f_a}{k_f}$.

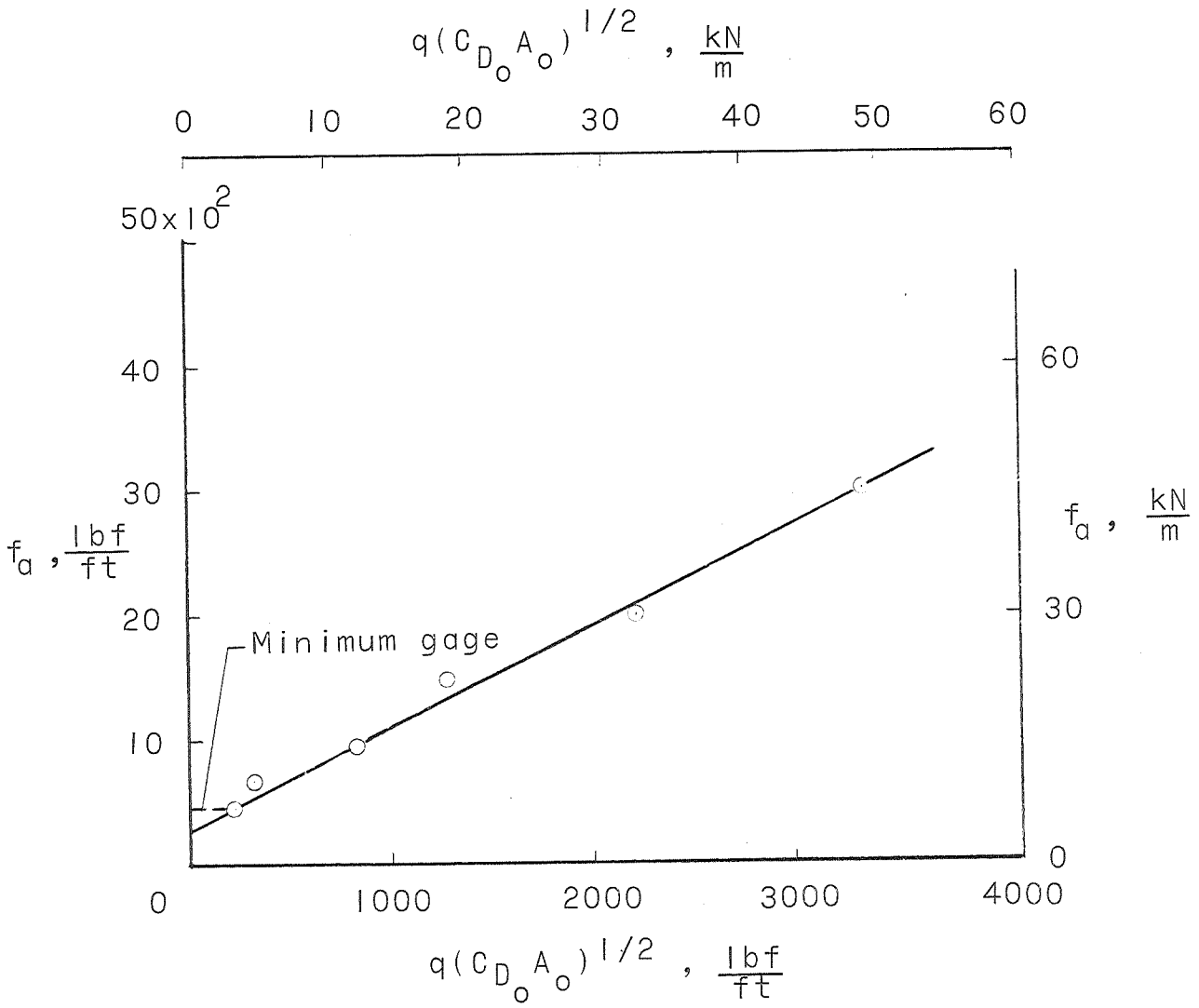

(b) Ringsail.

Figure 3.- Continued.

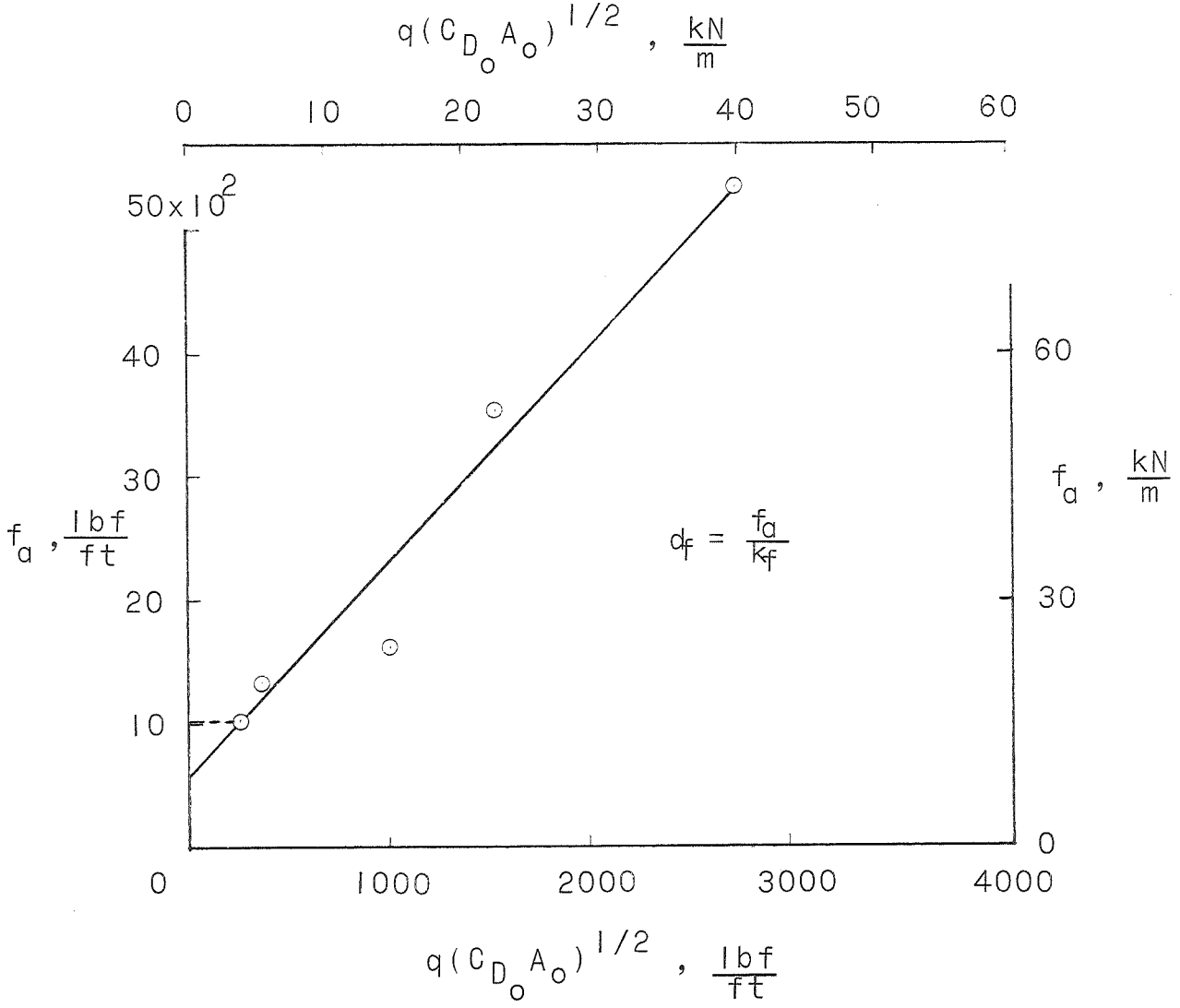

(c) Hemisflo.

Figure 3.- Continued.

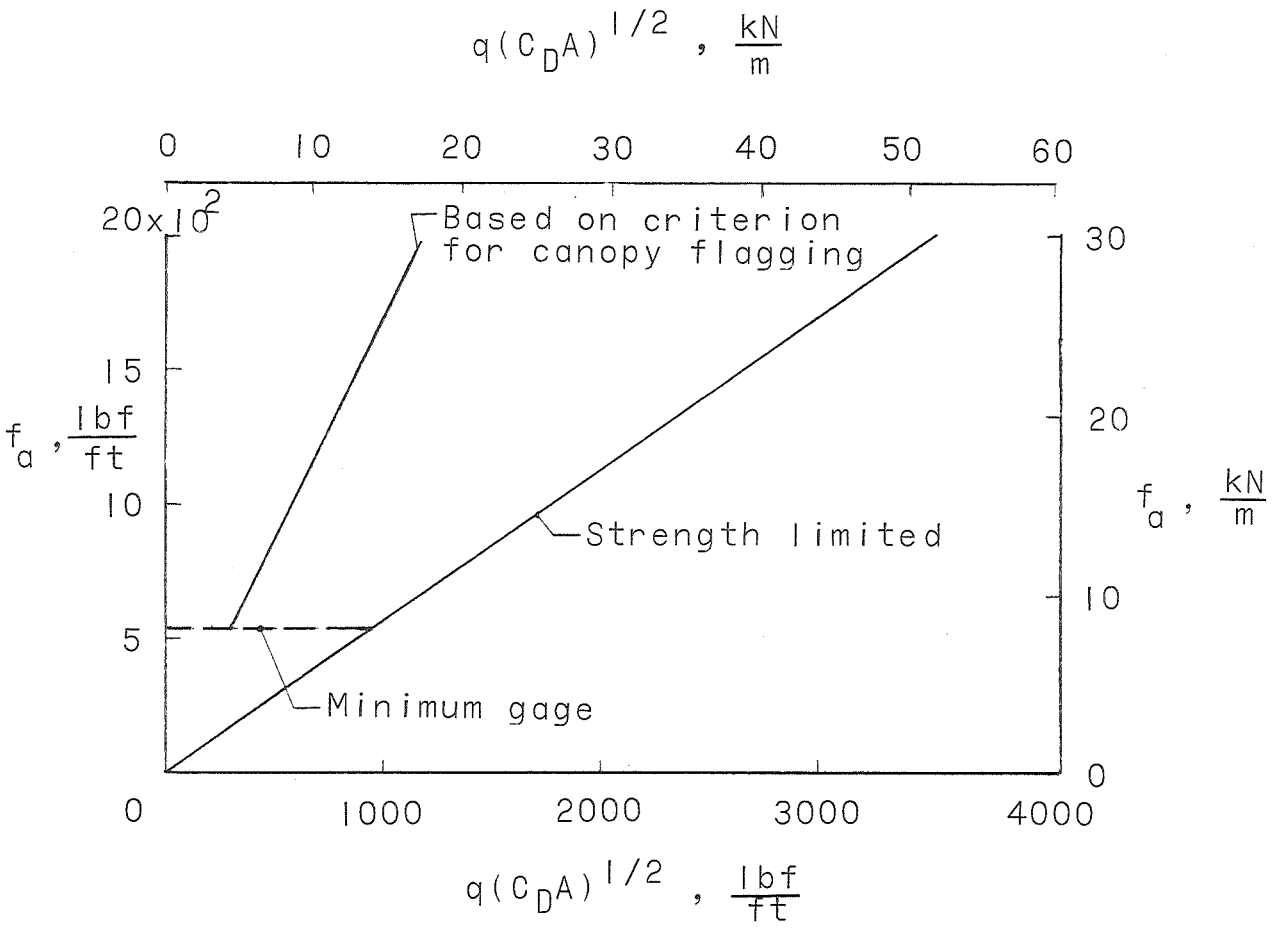

(d) Ballute.

Figure 3.- Continued.

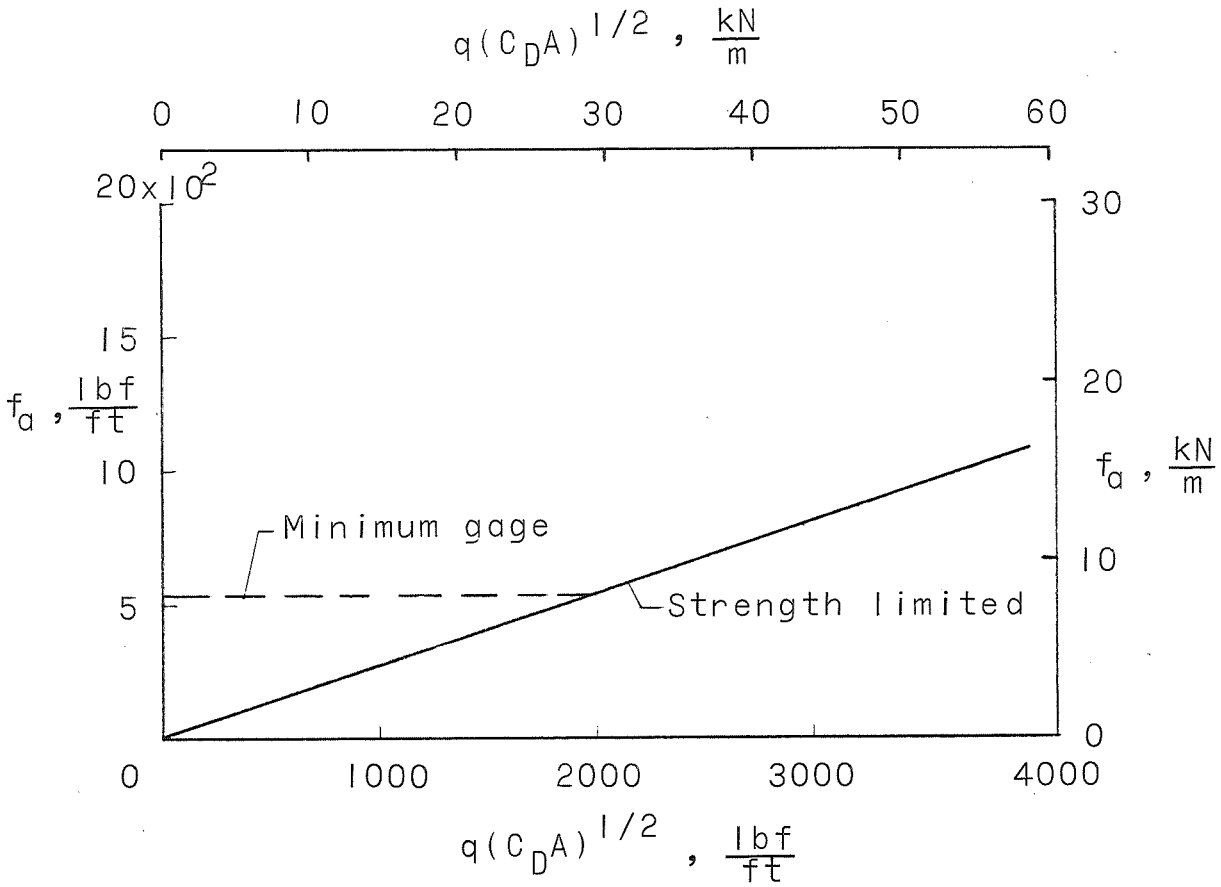

(e) AID.

Figure 3.- Concluded.

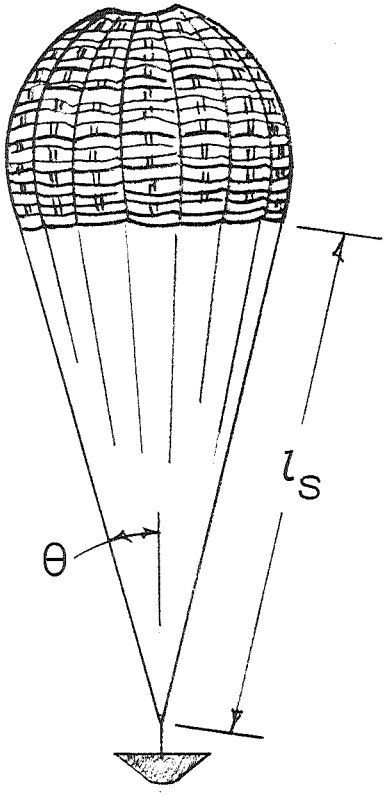

Modified
Hemisflo

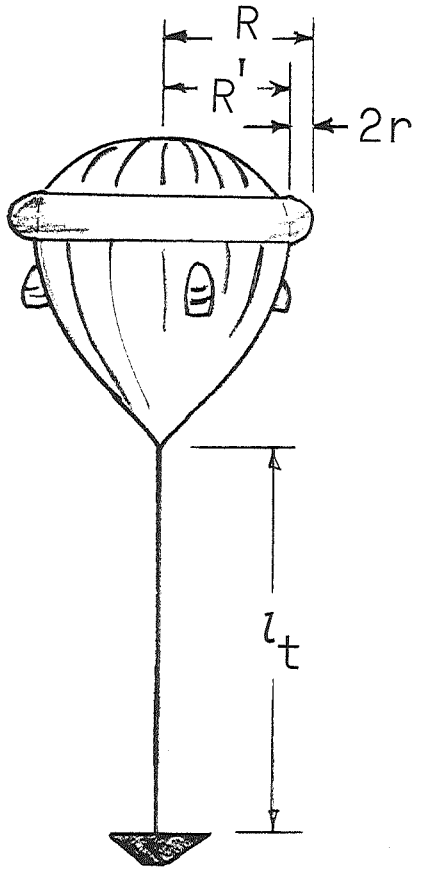

Ballute

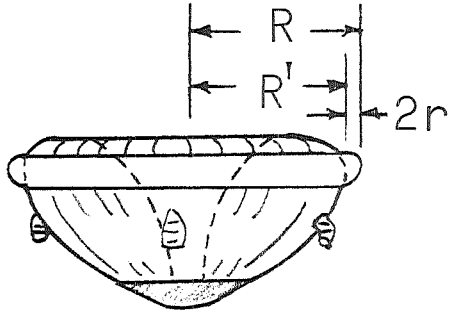

Attached
Inflatable
Decelerator

Figure 4.- Supersonic decelerators.

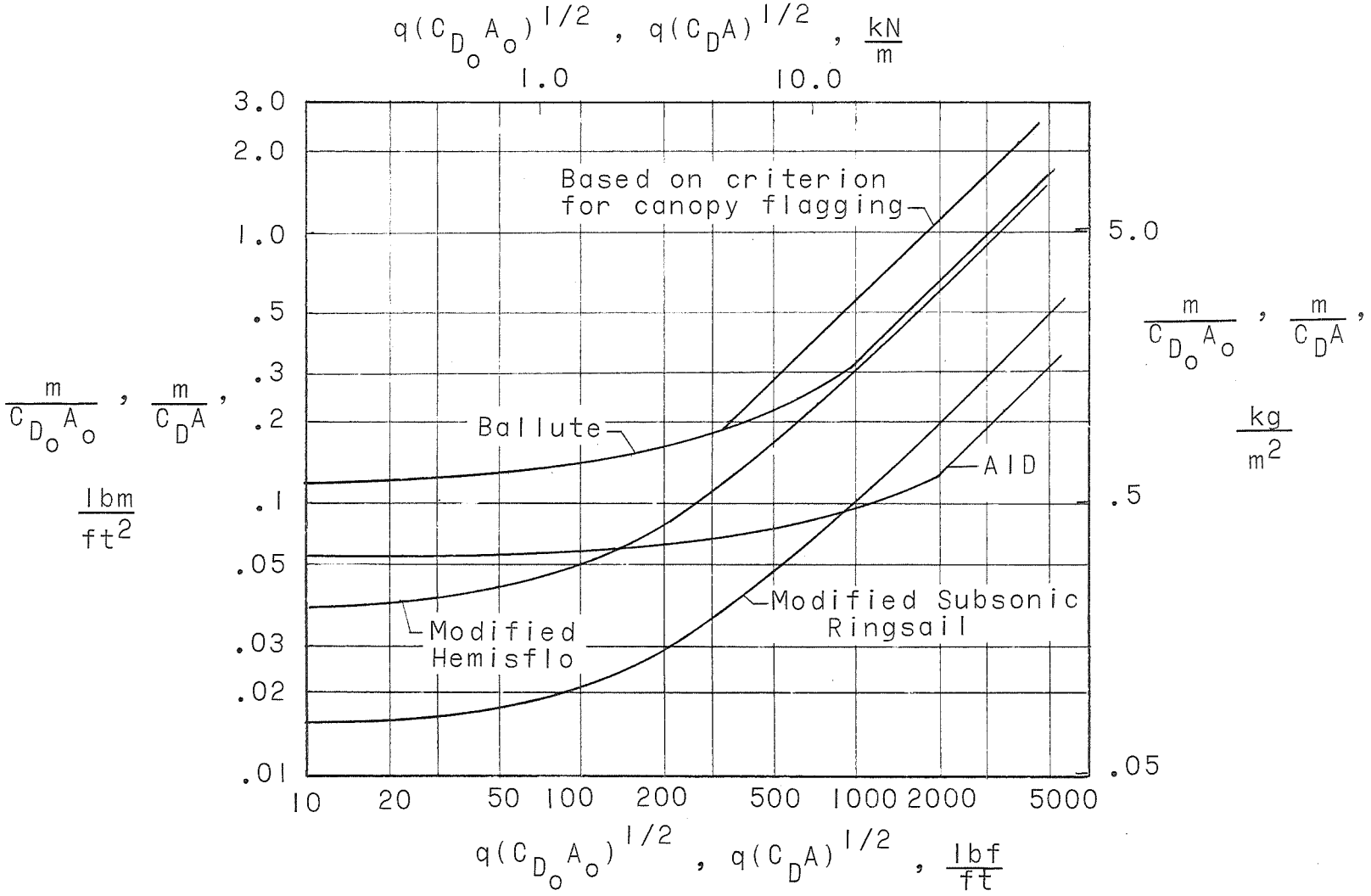

Figure 5.- Merit function for supersonic decelerators.

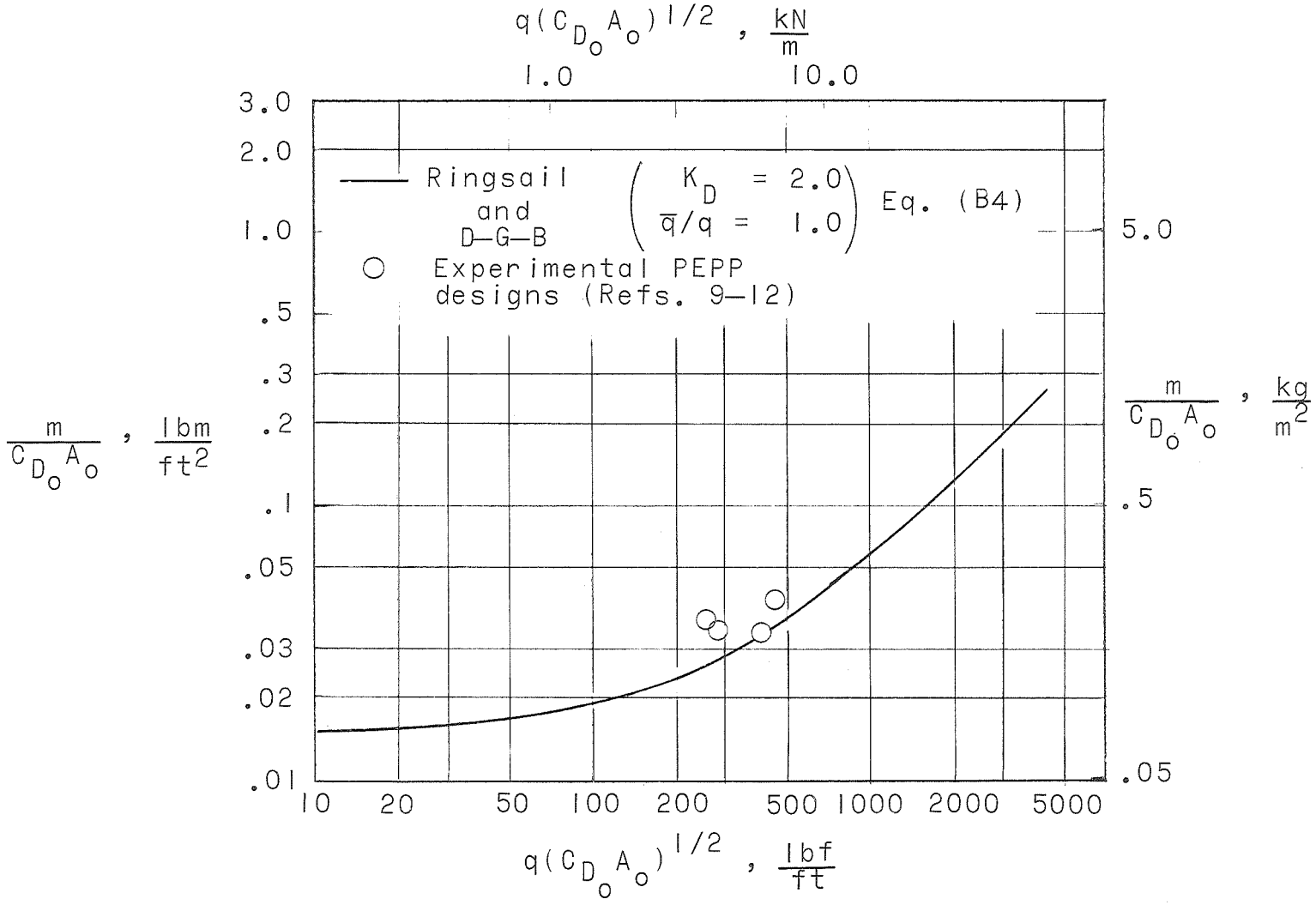

Figure 6.- Comparison of recent ringsail and D-G-B designs with merit function.

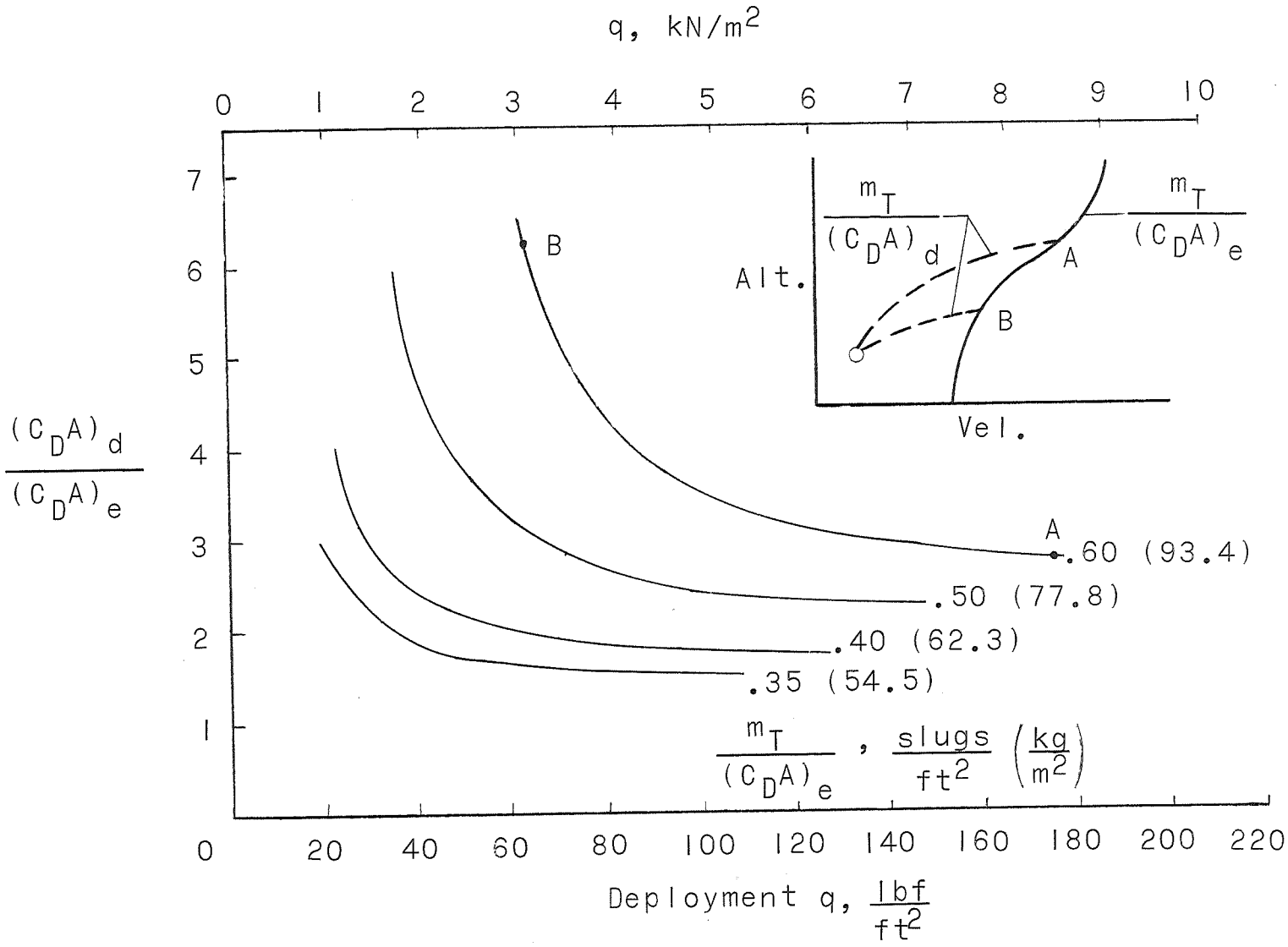

Figure 7.- Decelerator area required to achieve condition of Mach 1 at altitude of 15 000 ft (4570 m) and entry velocity of 12 000 ft/sec (3660 m/s). (VM-8 atmosphere of ref. 13.)

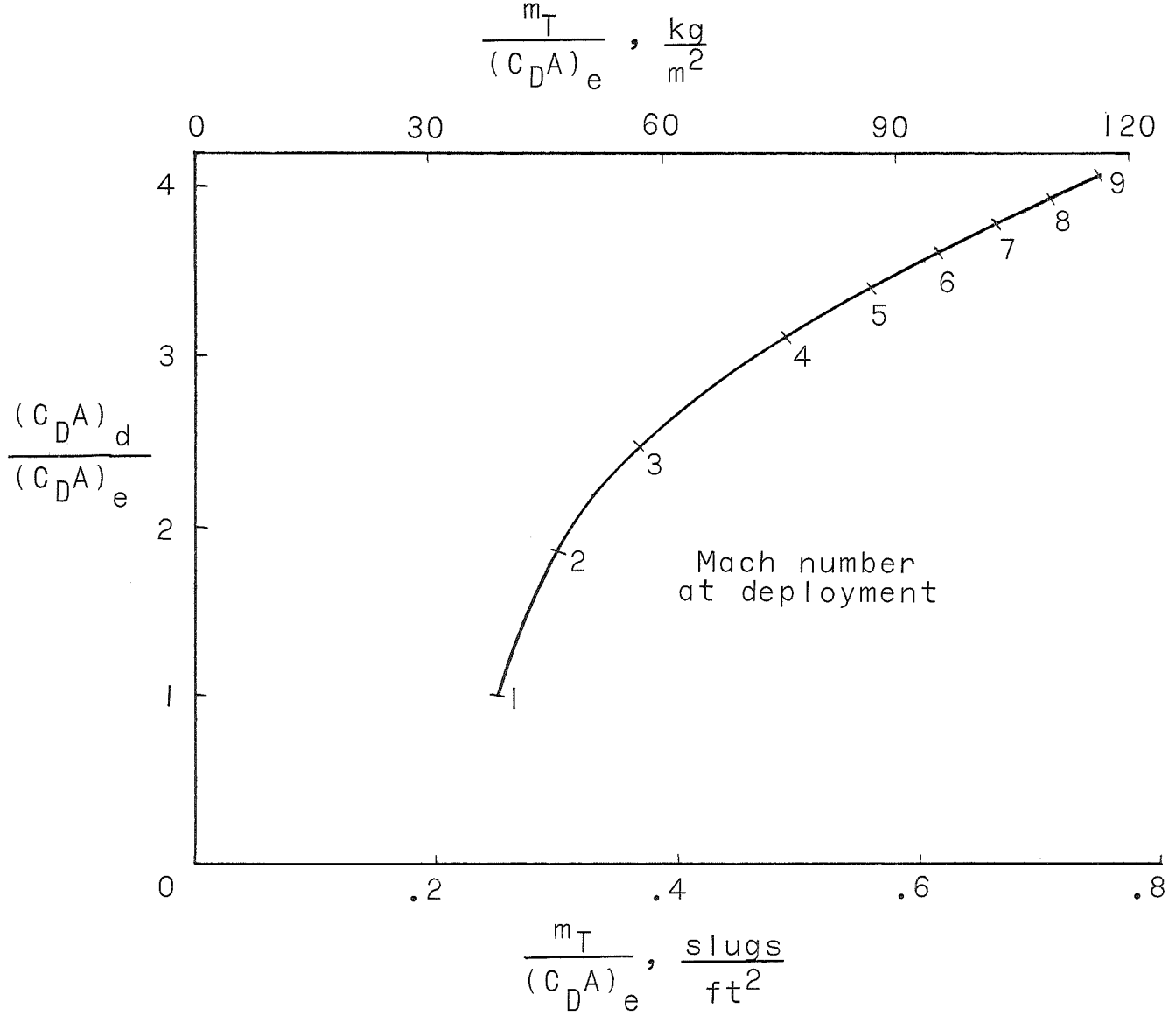

Figure 8.- Optimum decelerator area as a function of entry ballistic coefficient.

NATIONAL AERONAUTICS AND SPACE ADMINISTRATION
WASHINGTON, D. C. 20546

OFFICIAL BUSINESS

FIRST CLASS MAIL

POSTAGE AND FEES PAID
NATIONAL AERONAUTICS AND
SPACE ADMINISTRATION

POSTMASTER: If Undeliverable (Section 158 Postal Manual) Do Not Return

---

"The aeronautical and space activities of the United States shall be conducted so as to contribute . . . to the expansion of human knowledge of phenomena in the atmosphere and space. The Administration shall provide for the widest practicable and appropriate dissemination of information concerning its activities and the results thereof."

— NATIONAL AERONAUTICS AND SPACE ACT OF 1958

NASA SCIENTIFIC AND TECHNICAL PUBLICATIONS

TECHNICAL REPORTS: Scientific and technical information considered important, complete, and a lasting contribution to existing knowledge.

TECHNICAL NOTES: Information less broad in scope but nevertheless of importance as a contribution to existing knowledge.

TECHNICAL MEMORANDUMS: Information receiving limited distribution because of preliminary data, security classification, or other reasons.

CONTRACTOR REPORTS: Scientific and technical information generated under a NASA contract or grant and considered an important contribution to existing knowledge.

TECHNICAL TRANSLATIONS: Information published in a foreign language considered to merit NASA distribution in English.

SPECIAL PUBLICATIONS: Information derived from or of value to NASA activities. Publications include conference proceedings, monographs, data compilations, handbooks, sourcebooks, and special bibliographies.

TECHNOLOGY UTILIZATION PUBLICATIONS: Information on technology used by NASA that may be of particular interest in commercial and other non-aerospace applications. Publications include Tech Briefs, Technology Utilization Reports and Notes, and Technology Surveys.

Details on the availability of these publications may be obtained from:

SCIENTIFIC AND TECHNICAL INFORMATION DIVISION

NATIONAL AERONAUTICS AND SPACE ADMINISTRATION

Washington, D.C. 20546